

GPO PRICE \$ \_\_\_\_\_

CSFTI PRICE(S) \$ \_\_\_\_\_

Hard copy (HC) \_\_\_\_\_

Microfiche (MF) \_\_\_\_\_

ff 653 July 65

DEVELOPMENTS IN UPPER ATMOSPHERIC  
SCIENCE DURING THE IQSY

by

Francis S. Johnson  
Southwest Center for Advanced Studies  
Dallas, Texas

Presented at the

Symposium on the Years of the Quiet Sun - IQSY  
National Academy of Sciences  
104th Annual Meeting

April 24 - 27, 1967  
Washington, D. C.



To be Published in

Proceedings of the National Academy of Sciences

FACILITY FORM 602	N 68-34680	
	(ACCESSION NUMBER)	(THRU)
	12	1
	(PAGES)	(CODE)
CR-86846	13	
(NASA CR OR TMX OR AD NUMBER)	(CATEGORY)	

DEVELOPMENTS IN UPPER ATMOSPHERIC  
SCIENCE DURING THE IQSY

by


Francis S. Johnson  
Southwest Center for Advanced Studies  
Dallas, Texas

During the IQSY, there were of course many advances in the area of upper atmospheric science, and it would take a great deal of time and space to describe them all adequately. It is therefore necessary to arbitrarily select just a few of the advances that were, in my view, among the more important.

Neutral Upper Atmosphere

The vertical structure of the atmosphere is in large degree controlled by its temperature distribution, and the largest variations in temperature occur above 200-km altitude. This is illustrated in Figure 1, which shows a typical temperature distribution up to 100 km, and three distributions at higher altitudes. The three distributions shown indicate near-extreme conditions and an in-between, or average, situation. The range of variation can be seen to be very great, far over a factor of two at the highest altitudes. The biggest portion of the variation is governed by the solar cycle, the highest temperatures occurring near sunspot maximum. The constant temperatures above about 300 km is frequently referred to as the exospheric temperature.

The total amount of atmosphere above any location on the earth's surface at sea level, as indicated by the barometric pressure, is nearly constant (within about 5% of its mean value); this near constancy apparently



results from the meteorological circulation of the lower atmosphere. The vertical extension of the atmosphere is governed by its temperature and molecular weight. Where the temperature is high, the atmosphere is more extended in the vertical direction than where it is not. The effect of temperature becomes especially pronounced above 100 km, where the extreme variations indicated in Figure 1 occur. Part of the variation shown in Figure 1 is a diurnal variation, where the afternoon exospheric temperature maximum is about 30% greater than the nighttime minimum. This causes the atmosphere to develop an afternoon bulge that affects satellite orbital decay. Several people have mapped the afternoon bulge making use of satellite orbital decay data. Figure 2 shows a result obtained by Jacchia (1964) for the northern hemisphere summer. This shows the bulge lagging about two hours behind the subsolar point on the earth's surface. The concept was that the bulge moved back and forth across the equator with season, following the overhead sun in latitude, but lagging about two hours behind it. This roughly describes the thermal structure of the upper atmosphere as it was understood at the beginning of the IQSY.

The early mapping of the diurnal bulge was accomplished using data from relatively low inclination satellites, so the north-south extent of the bulge was not precisely determined. Data from the higher inclination orbits of Injun 3 ( $70^{\circ}$  inclination, 250 km apogee), and Explorers 19 ( $17.6^{\circ}$ , 592 km) and 24 ( $81.4^{\circ}$ , 526 km) became available during the IQSY. At first the new data did not clarify the situation. Jacchia and Slowey (1966) decided on the basis of the new data that the diurnal bulge remained centered on the geographic equator, but that it was considerably elongated in the north-south direction. The analysis was made difficult by the circumstance

that the periods for the precession of the apogees around the orbits were nearly a year or half-a-year for the satellites concerned, making them relatively poorly suited for the separation of any seasonal effects from an elongation of the bulge in the north-south direction.

Anderson (1966) has argued that the upper atmospheric densities are much greater over the summer polar region than over the winter polar region, which is inconsistent with Jacchia and Slowey's conclusion. Although Anderson's conclusion sounds eminently plausible on the basis of solar heating of the upper atmosphere, his presentation of data does not provide very convincing support for his hypothesis. Further, Keating and Prior (1966) reached a still different conclusion. On the basis of data from Explorers 19 and 24, they at first concluded that the diurnal bulge is in the winter hemisphere. Although at first they believed on this basis that the temperature maximum occurs in the winter hemisphere, they later concluded, using additional data from Explorer 9 and Echo 2, that the winter bulge is due to increased helium content in the winter upper atmosphere, and that the temperature maximum occurs in the summer hemisphere in accordance with earlier concepts (Keating and Prior, 1967). This is basically a reasonable suggestion that can be understood in terms of the physics that controls the composition of the upper atmosphere; the necessary concepts will be discussed next.

Up to an altitude of about 100 km, the atmosphere is generally well mixed, but at higher altitudes it tends to be in a condition of diffusive equilibrium in the gravitational field. With diffusive equilibrium, each atmospheric constituent is distributed independently of the others. The atmosphere reaches this condition when it is mixed infrequently enough to permit molecular diffusion to accomplish this result, and this occurs preferentially at high altitudes because the molecular diffusion coefficient

varies inversely as the atmospheric density and hence increases exponentially with altitude. Between the well mixed region of the atmosphere and the diffusive equilibrium region, there is a transition region in which the effects of mixing compete with those of molecular diffusion. Above the transition region, molecular diffusion dominates over the mixing, and below the transition region, mixing dominates over molecular diffusion. This is concisely stated by saying that the molecular diffusion coefficient is much larger than the eddy diffusion coefficient above the transition region, and vice versa below it; in the transition region they are comparable. Sometimes the altitude at which they are equal is called the turbopause, indicating that at this altitude turbulence ceases to be important in many atmospheric phenomena. From information on heat transfer in the atmosphere, it appears that eddy diffusion also increases exponentially with altitude, but at a much slower rate than molecular diffusion. Between 15 km and 105 km, eddy diffusion increases from about  $10^4$  to  $10^7$   $\text{cm}^2/\text{sec}$ , or three orders of magnitude, while molecular diffusion increases by six orders of magnitude over this altitude range.

Figure 3 shows typical distributions of atmospheric constituents in the diffusive equilibrium condition. Note that the slopes vary inversely with the atomic weight, as each constituent is distributed in the gravitational field independently of the others, and the light constituents fall off with altitude less rapidly than the heavy constituents. The concentrations shown are for conditions near the minimum of the solar cycle. As the slopes are changed to correspond to different temperatures, the curves more or less rotate about their lower end points; the relative change in concentration at the higher altitudes for a given change in temperature is much smaller

for the distributions whose slopes are steep than for distributions whose slopes are small. As a result, densities just below 500 km, where atomic oxygen is the principal constituent, change much more than just above 500 km, where helium is the principal constituent. It was just this effect which led to the recognition of the importance of helium in the upper atmosphere by Nicolet (1961), at which time the transition between atomic oxygen and helium occurred at a somewhat higher altitude than occurs near solar minimum. A constituent which is so light that its concentration falls very slowly with altitude cannot have its concentrations at very high altitudes greatly increased by increasing its already large slope and while keeping the low altitude concentration unchanged. The atomic hydrogen distribution has not been shown in Figure 3, but it is probably the principal atmospheric constituent above about 700 km.

Figure 4 shows distributions of atmospheric constituents in the lower part of the diffusive equilibrium region and in the transition region. Distributions are shown for atomic and molecular oxygen, molecular nitrogen, helium, and argon where the eddy mixing coefficient is  $5 \times 10^6 \text{ cm}^2 \text{ sec}^{-1}$ . Also shown by dashed curves are distributions for helium and argon where the eddy mixing coefficient is  $5.5 \times 10^5 \text{ cm}^2 \text{ sec}^{-1}$ ; note the factor of 5 increase in helium and factor of 2 decrease in argon at the higher altitudes when the eddy mixing coefficient is reduced. The relative distributions of argon and helium are unchanged in the diffusive equilibrium region, and the same factors apply at all altitudes since the same vertical temperature distribution was assumed for the two different rates of eddy mixing. By contrast, if a temperature change in the thermosphere were assumed, the changes in concentration of each species would change with altitude. With a  $100^\circ\text{K}$  change above

200 km decreasing to no change at 120 km, the distributions are not changed perceptibly below about 250 km, but noticeably changes occur at 300 km and greater changes occur at higher altitudes.

The changes that may occur in the winter hemisphere can be described in terms of the distributions shown in Figure 4. The helium and argon concentrations associated with the lesser eddy mixing coefficient may apply in the winter polar region; this would occur if the lower thermosphere (80-100 km) is less turbulent in winter than in summer. Even if the temperature is somewhat lower in the winter hemisphere, the increased helium concentration could still cause the maximum density of the atmosphere at altitudes above 500 km to occur in the winter hemisphere. At altitudes below 500 km, where the atomic oxygen concentrations dominate over helium and control the atmospheric density, the maximum densities would occur in the summer hemisphere where the temperature maximum occurs. Near sunspot maximum, the transition altitude to helium is much higher, perhaps 1000 km, and the winter bulge would be confined to this higher altitude region.

Distributions for atomic and molecular oxygen calculated using the lower value of  $5.5 \times 10^5 \text{ cm}^2 \text{ sec}^{-1}$  for the eddy mixing coefficient are not shown in Figure 4. A lesser mixing rate would allow a greater degree of oxygen dissociation to occur, with increased atomic and decreased molecular concentrations, provided the rate of photodissociation were unchanged. This arises because the pattern of behavior is for eddy mixing to transport molecular oxygen upward into the regions where it is photodissociated; the reaction rates for recombination of atoms into molecules are too slow to permit recombination to occur at the altitudes where photodissociation occurs, and molecular diffusion and eddy mixing must transport the atomic oxygen downward into regions of greater atmospheric concentration where re-

combination can take place. Obviously, due to the lesser sunlight, the rates of photodissociation must decrease in the winter hemisphere, acting to decrease the atomic oxygen concentration and increase the molecular oxygen concentrations. The consequences of this cannot at present be calculated, because horizontal transport acts to maintain the degree of oxygen dissociation, and the rates of horizontal transport are not known. Some rocket and satellite measurements suggest that the degree of dissociation at 120 km does not change greatly with latitude and season, so only the atomic and molecular oxygen calculations calculated on the basis of an eddy mixing rate of  $5 \times 10^6 \text{ cm}^2 \text{ sec}^{-1}$  are shown in Figure 4, as these results are in fair agreement with the observations. At the present time, these are our best estimates of the vertical distributions of atomic and molecular oxygen over the winter polar region.

### Ionosphere

#### (a) Improved Morphology

During the IQSY, an improved description of the general pattern of ionospheric behavior has emerged. Although several new features have been observed or better defined, there has not been a corresponding improvement in the understanding of the physical causes of those new features. There have been notable improvements during the IQSY in the physical understanding of some physical features of the ionosphere, but these generally were features that were well described before the IQSY; some of these will be discussed later on.

Although the atmosphere is generally well stratified, so that changes in the horizontal direction take place only slowly, and solar radiation falls uniformly on the earth, there are sometimes some surprisingly rapid changes



in ionization with location over the earth's surface. Muldrew (1965) has described an east-west trough of greatly depressed F-region electron concentration that occurs at night near a geomagnetic latitude of  $60^{\circ}$ . Figure 5 shows Muldrew's results. At higher latitude, some narrower troughs sometimes exist, also indicated in Figure 5, but the one near  $60^{\circ}$  geomagnetic latitude (about  $45^{\circ}$  geographic latitude near  $75^{\circ}$ W longitude where these observations were made) is a particularly regular phenomenon. Data on this trough have been acquired primarily from polar-orbit topside-sounder satellites. There is no general agreement as to the cause of this trough, but it is probably due to a persistent pattern in the upper atmospheric wind system.

Another sudden drop in electron and ion concentration has been observed in the magnetosphere, well above the ionosphere. Carpenter (1966) has found from radio whistler data that the electron concentration often falls suddenly from a value near  $100 \text{ cm}^{-3}$  to less than  $1 \text{ cm}^{-3}$ ; the place where this occurs is usually referred to as the "whistler knee" or "plasmopause", and it frequently occurs near the magnetic field line that leaves the earth near a geomagnetic latitude of  $60^{\circ}$ . This suggests that the geomagnetic field is only partially filled with thermal plasma, as indicated in Figure 6. The portion of the geomagnetic field containing thermal plasma is called the plasmasphere, and its outer boundary is the plasmopause; the region just beyond the plasmopause joins, at least roughly, to the nighttime trough in F region ionization. Carpenter has also recognized a pattern of diurnal motion for the plasmopause, and this is shown in Figure 7. There is a slow inward nighttime movement, providing a minimum geocentric distance near dawn, followed by a slight outward movement during the morning and early

afternoon and then a rapid outward shift in the late afternoon. The dashed line in Figure 7 shows the approximately six-hour period of rapid variation during which the details of motion are not well known. During periods of geomagnetic activity, the plasmapause position moves inward with at most a few hours delay. The region in Figure 7 bounded by the crosses is that within which a significant number of observations has been made - it does not represent a physical boundary. Carpenter interprets a portion of the plasmapause motion as due to plasma drift under action of an electric field. However, the absence of plasma beyond the plasmapause remains essentially unexplained.

Another strange property of the ionosphere is the presence of irregularities with scale sizes ranging from possibly a few meters to a few tens of kilometers. Calvert and Van Zandt (1966) have measured some of these irregularities in a satellite and have found depressions in electron concentration of a few percent over distances of a few kilometers. Such irregularities must have a field aligned structure, and they are presumably responsible for the guidance of radio whistlers from hemisphere to hemisphere along the magnetic field lines. Such ducting of radio waves has also been observed at high frequency (Van Zandt et al., 1965).

(b) Diffusion and Drift

Probably the most significant increases in ionospheric understanding that have occurred recently have involved plasma diffusion and drift under the action of electric fields. Three particularly significant advances involve the formation of the equatorial anomaly in the F region, the persistence of the F region at night, and the formation of mid-latitude sporadic E layers.

The maximum electron concentrations in the F region do not occur at the equator, but on either side of the geomagnetic equator. A rather pronounced trough or relative minimum exists along the geomagnetic equator during

the afternoon, and the regions of maximum electron concentration occur as two somewhat elongated maxima symmetrically located about  $15^{\circ}$  north and south of the geomagnetic equator. Hanson and Moffett (1966) have explained this in terms of an eastward directed electric field that produces an upward drift of ionospheric plasma of about  $10 \text{ m sec}^{-1}$ . The plasma then diffuses downward in the gravitational field along the geomagnetic equator towards higher latitudes. Figure 8 shows the pattern of transport, and Figure 9 shows the calculated ionization contours when photoionization, recombination, diffusion and electromagnetic drift are taken into account for daytime conditions near the minimum of the solar cycle.

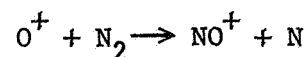
The F region persists throughout the night. To explain this in terms of recombination processes, the rate coefficients would have to be unreasonably small. Hanson and Patterson (1964) showed how the F region could be maintained through the course of the night with acceptable rate coefficients provided an electric field were present that would cause an upward drift; the lesser densities that prevail at the higher altitudes reduce the loss rate to a value that is consistent with the nighttime persistence of the F region. This also provides a ready explanation for the F region trough at  $60^{\circ}$  geomagnetic latitude if there is a mechanism to reverse the electric field direction there. Since the electric fields are generated by motions arising in the neutral atmosphere, the question resolves itself into one of a pattern of atmospheric circulation.

Sporadic E at temperate latitude has been identified as consisting of thin layers of greatly enhanced electron concentration, as indicated in Figure 10 (Smith, 1966). A mechanism to explain the formation of such a layer has been recognized by Axford and Cunnold (1966). This depends upon

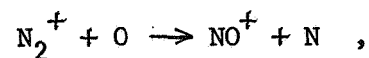
the existence of a strong wind shear that causes the plasma above and below the shear to drift into the shear zone and increase in concentration there. Where several ion species are present, the more rapidly combining species are preferentially removed by recombination in the region of the concentration increase, leaving the most slowly recombining species as the principal ion constituents in the thin sporadic E layer. The most slowly recombining ions in the ionosphere are metallic ions, probably of meteoric origin, but they are normally of relatively minor importance. However, they become the predominant ion in the sporadic E layer because of the selective removal of the ions that normally predominate in the E region - molecular oxygen and nitric oxide.

(c) Chemistry

There has been frequent disagreement in past years between recombination rates and reaction rates derived from ionospheric data and those obtained from laboratory measurements for reactions that were thought to be pertinent. Norton et al. (1963) have presented ionospheric evidence for reaction rates; in particular they noted the importance of the reaction



and that its reaction rate should be near  $10^{-12} \text{ cm}^3 \text{ sec}^{-1}$ . This has now been confirmed by laboratory measurements by Ferguson et al. (1965a), who obtained a value of  $3 \times 10^{-12} \text{ cm}^3 \text{ sec}^{-1}$ . Ferguson et al. (1965b) have also measured the rate for the reaction



obtaining a value of  $2.5 \times 10^{-10} \text{ cm}^3 \text{ sec}^{-1}$ ; this is the main loss process for  $N_2^+$  between 120 and 220 km, and it provides the main source of  $NO^+$  near 140 km.

## Plasma Properties

### (a) Ion Whistlers

Ion cyclotron whistlers have been observed in satellites (Gurnett et al., 1965). These are signals that propagate below the ion gyro frequency in the left-handed polarized mode. An example is shown in Figure 11. The electron whistler in Figure 11 is a short fractional-hop electron whistler propagating in the right-hand polarized whistler mode. At a cross-over frequency that occurs below the proton gyro frequency, the upgoing right-hand polarized whistler signal undergoes a polarization reversal to become a proton cyclotron whistler. Because of the presence of heavier ions that would not permit the propagation of ion cyclotron waves with frequencies greater than the heavy ion cyclotron frequency, the mode can be excited only by the polarization reversal mechanism at the cross-over frequency. In common with other whistlers, the maximum frequency is the gyro frequency.

### (b) Plasma Line Observation in Thomson Scatter

Incoherent radar backscatter, or Thomson scatter, from the ionosphere can be observed when powerful transmitters are used at frequencies far above the plasma frequency of the ionosphere. Most of the returned energy is in a narrow central line where the line width is governed by the Doppler spread for the ion thermal velocities. However, a small amount of power is returned in a pair of sharp lines separated from the transmitter frequency by the plasma frequency. This has been observed by Perkins, Salpeter and Yngvesson (1965), and their results are shown in Figure 12. A filter is used which is offset from the transmitter frequency by the indicated amount. Two regions, one above the ion concentration maximum and one below it, give responses that fall within the bandpass of the filter, so two peaks are seen.

## REFERENCES

- Anderson, A. D., An Hypothesis for the Semi-Annual Effect Appearing in  
Satellite Orbital Decay Data, Planet. Space Sci., 14, 849-861, 1966
- Axford, W. I. and D. M. Cunnold, The Wind Shear Theory of Temperature Zone  
Sporadic E, Radio Science, 1 (New Series), 191-198, 1966
- Calvert, W. and T. E. Van Zandt, Fixed Frequency Observation of Plasma  
Resonances in the Topside Ionosphere, J. Geophys. Research, 71,  
1799-1813, 1966
- Carpenter, D. L., Whistler Studies of the Plasmopause in the Magnetosphere -  
1: Temporal Variations in the Position of the Knee and Some Evidence  
on Plasma Motions near the Knee, J. Geophys. Research, 71, 693-709, 1966
- Carpenter, D. L., N. Dunckel, and J. Walkup, A New Phenomenon: Whistlers  
Trapped Below the Protonosphere, J. Geophys. Research, 69, 5009-5018,  
1964
- Ferguson, E. E., F. C. Fehsenfeld, P. D. Golden and A. L. Schmeltekopf,  
Positive Ion-Neutral Reactions in the Ionosphere, J. Geophys. Research,  
70, 4323-4329, 1965a
- Ferguson, E. E., F. C. Fehsenfeld, P. D. Golden, A. I. Schmeltekopf and  
H. I. Schiff, Laboratory Measurements of the Rate of the Reaction  
 $N_2^+ + O \rightarrow NO^+ + N$  at Thermal Energy, Planet. Space Sci., 13, 823-827,  
1965b
- Gurnett, D. A. and S. D. Shawhan, Ion Cyclotron Whistlers, J. Geophys. Research,  
70, 1665-1688, 1965
- Hanson, W. B. and R. J. Moffett, Ionization Transport Effects in the  
Equatorial F Region, J. Geophys. Research, 71, 5559-5572, 1966

The response seen in Figure 12 is greater than predicted by the theory for a thermal plasma. Perkins and Salpeter (1965) have explained the enhancement in terms of photoelectrons. Recently, they have observed differences between the upshifted and the downshifted frequencies that result from the greater number of upward moving (escaping) photoelectrons than downgoing photoelectrons that have come from the magnetically conjugate point in the other hemisphere; this observation indicates that there is significant scattering of photoelectrons in the magnetosphere and that they cannot pass from one hemisphere to the other without significant attenuation.

This research was supported under National Aeronautics and Space Administration grant NsG-269.





- Hanson, W. B. and T. N. L. Patterson, The Maintenance of the Nighttime F-Layer, Planet. Space Sci., 12, 979-997, 1964
- Jacchia, L. G., The Temperature above the Thermopause, Smithsonian Astrophysical Observatory Special Report No. 150, 32 pp., 1964
- Jacchia, L. G. and J. Slowey, The Shape and Location of the Diurnal Bulge in the Upper Atmosphere, Smithsonian Astrophysical Observatory Special Report No. 207, 22 pp., 1966
- Keating, G. M. and E. J. Prior, Latitudinal and Seasonal Variations in Atmospheric Densities Obtained during Low Solar Activity by Means of the Inflatable Air Density Satellites, Seventh International Space Science Symposium of COSPAR, Vienna, 1966
- Keating, G. M. and E. J. Prior, The Distribution of Helium and Atomic Oxygen in the Exosphere, Spring Meeting, American Geophysical Union, Washington, D. C., 1967
- Muldrew, D. B., F-Layer Ionization Troughs Deduced from Alouette Data, J. Geophys. Research, 70, 2635-2650, 1965
- Nicolet, M., Helium, An Important Constituent of the Lower Exosphere, J. Geophys. Research, 68, 2263-2264, 1961
- Norton, R. B., T. E. Van Zandt and J. S. Denison, A Model of the Atmosphere and Ionosphere in the E and F<sub>1</sub> Regions, Proc. International Conference on the Ionosphere, ed. A. C. Strickland, Inst. Phys. and Phys. Soc. London, 26-34, 1963
- Perkins, F. W., and E. E. Salpeter, Enhancement of Plasma Density Fluctuations by Nonthermal Electrons, Phys. Rev., 139, A55-A62, 1965

- Perkins, F. W., E. E. Salpeter and K. O. Yngvesson, Incoherent Scatter  
from Plasma Oscillations in the Ionosphere, *Phys. Rev. Letters*, 14,  
579-581, 1965
- Smith, L. G., Rocket Observations of Sporadic E and Related Features of  
the E Region, *Radio Science*, 1 (New Series), 178-186, 1966
- Van Zandt, T. E., B. T. Leftres and W. Calvert, Explorer XX Observations  
at Conjugate Ducts, Report on Equatorial Aeronomy, ed. F. de Mendonca,  
325-327, 1965

#### FIGURE CAPTIONS

- Figure 1. Typical temperature distributions through the atmosphere representative of daytime conditions near solar maximum, nighttime conditions near solar minimum, and an in-between situation.
- Figure 2. The distribution of exospheric temperature over the earth during the northern hemisphere summer when the nighttime minimum temperature is  $1000^{\circ}\text{K}$  (after Jacchia, 1964).
- Figure 3. The distribution with altitude of atmospheric constituents in a condition of diffusive equilibrium. The distributions shown are representative of nighttime condition near solar minimum.
- Figure 4. The distributions with altitude of atmospheric constituents calculated taking into account molecular diffusion, eddy diffusion characterized by a coefficient equal to  $5 \times 10^6 \text{ cm}^2 \text{ sec}^{-1}$  (solid curves only), photodissociation of molecular oxygen, and recombination of atomic oxygen. The dashed curves show the calculated distributions of helium and argon taking into account molecular diffusion and eddy diffusion characterized by a coefficient equal to  $5.5 \times 10^5 \text{ cm}^2 \text{ sec}^{-1}$ .
- Figure 5. The maximum electron concentration in the ionosphere, expressed in terms of the plasma frequency in  $\text{Mc/s}$ , as a function of geographic latitude near  $75^{\circ}\text{W}$  longitude (after Muldrew, 1965).

- Figure 6. A typical boundary for the plasmopause as seen in meridional cross section (after Carpenter, 1966).
- Figure 7. The location of the plasmopause as seen in an equatorial cross section. The line of crosses does not represent a physical boundary; it only indicates the region within which a significant number of observations has been made (after Carpenter, 1966).
- Figure 8. The drift of ionospheric plasma near the geomagnetic equator calculated on the basis of diffusion and an eastward directed electric field (after Hanson and Moffett, 1966).
- Figure 9. Ionization contours near the equatorial anomaly of the ionospheric F region calculated on the basis of an eastward directed electric field when photoionization, recombination, diffusion, and electromagnetic drift are taken into account (after Hanson and Moffett, 1966).
- Figure 10. The ionization profile through a sporadic E layer at 113 km altitude (after Smith, 1966).
- Figure 11. The frequency-time characteristics of a proton whistler (after Gurnett et al., 1966).  $\Omega_1$  is the proton gyrofrequency and  $\Omega_{12}$  is the cross-over frequency.
- Figure 12. Plasma line observations in Thomson scatter (after Perkins et al., 1965). The responses shown are those obtained through filters offset from the transmitter frequency by the amounts shown. Two peaks are seen for each filter; these

come from the two regions, one above and one below the ionization maximum, where the plasma frequency equals the difference between the transmitter frequency and the filter frequency.

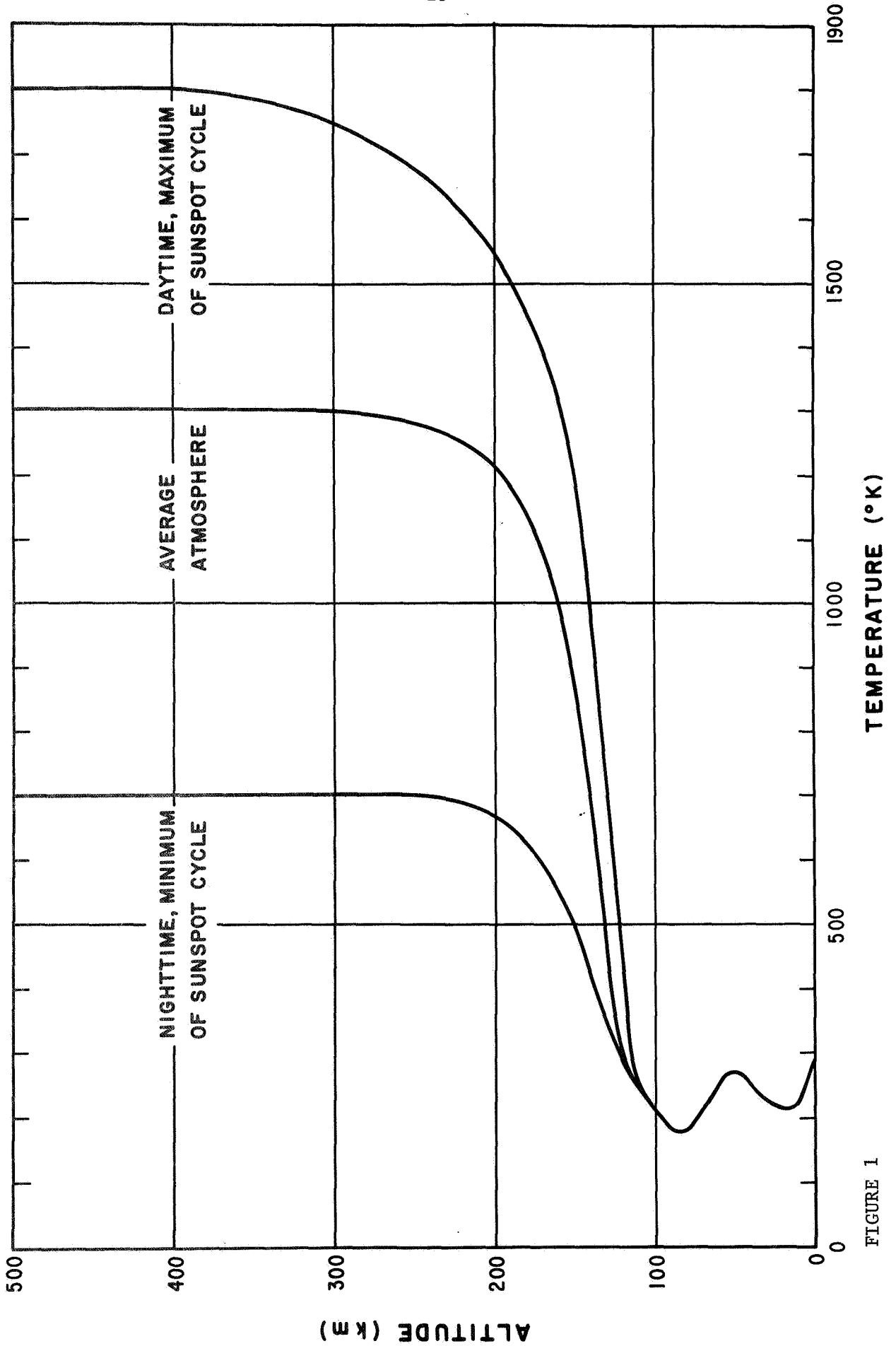


FIGURE 1

EXOSPHERIC TEMPERATURE DISTRIBUTION AT SUMMER SOLSTICE  
FOR  $T_e = 1000^\circ \text{K}$

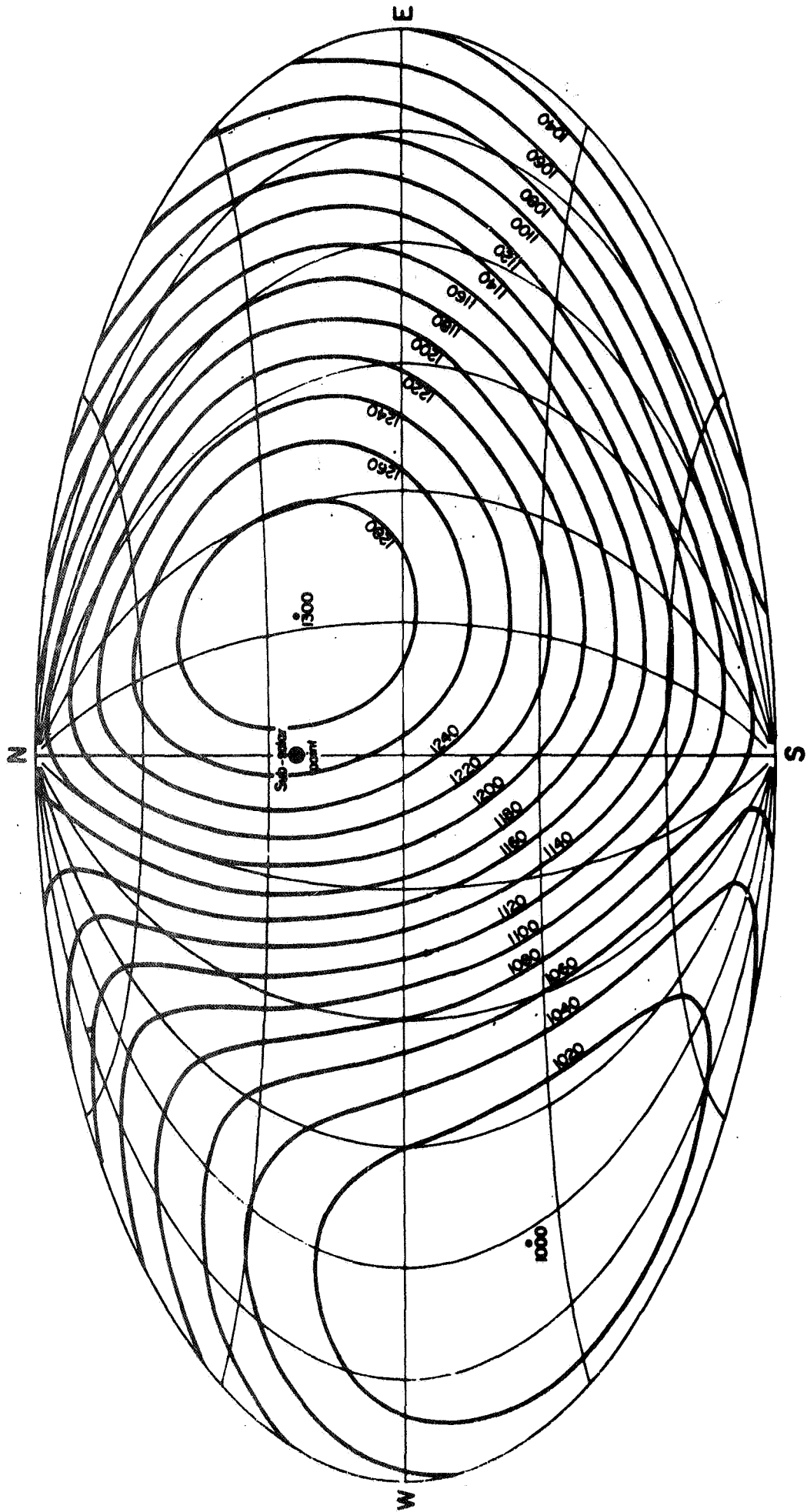


FIGURE 2

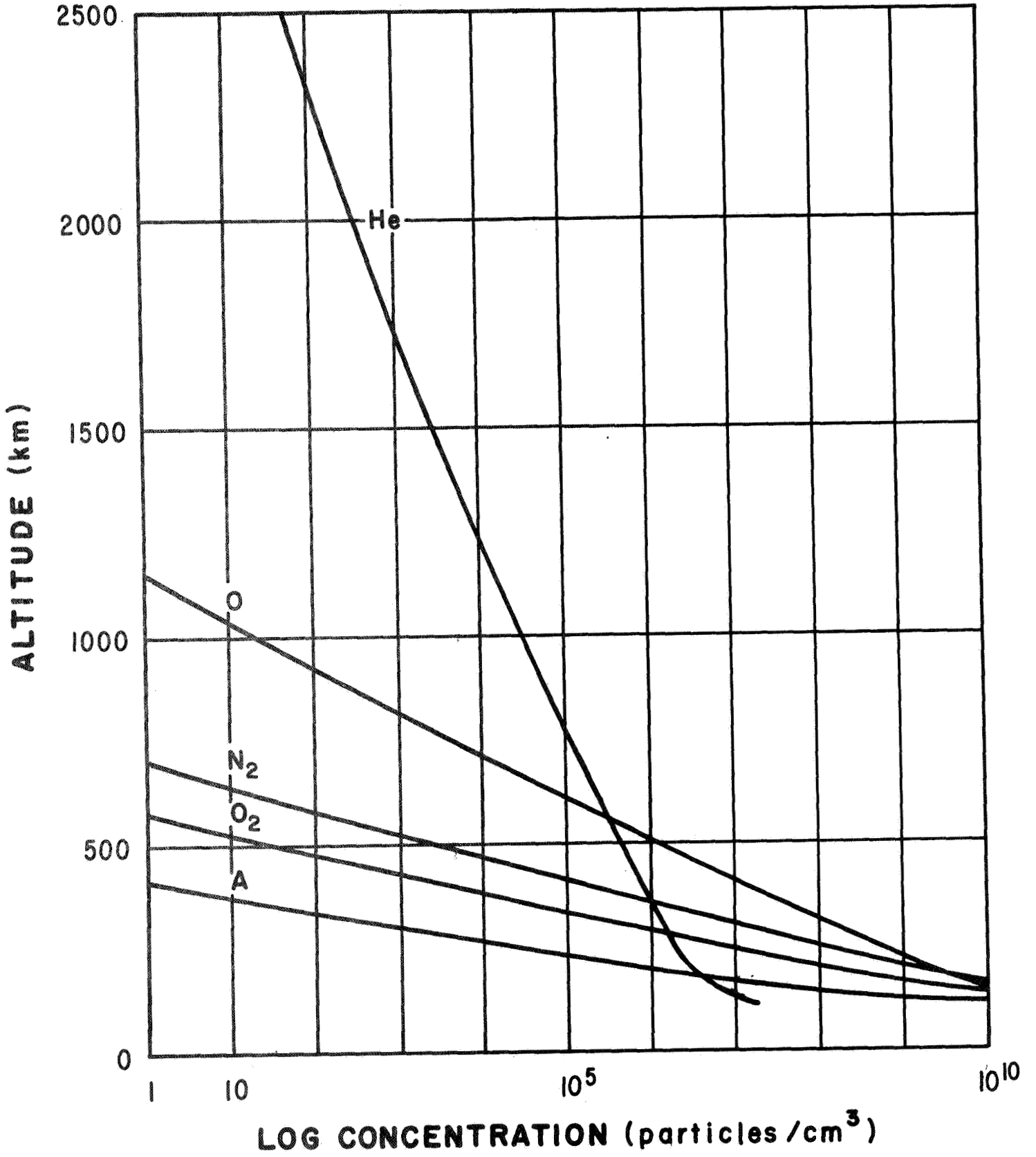


FIGURE 3



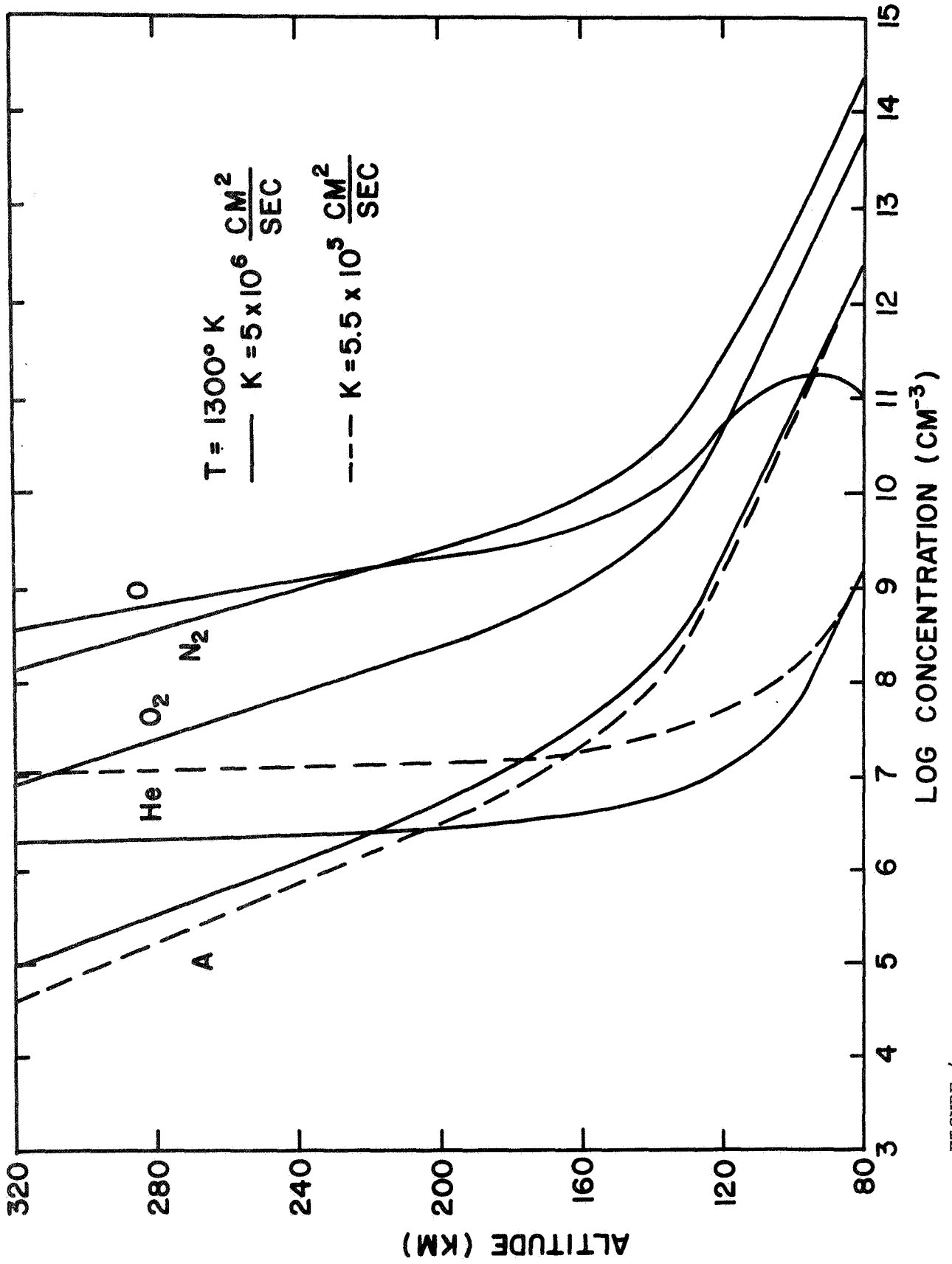


FIGURE 4

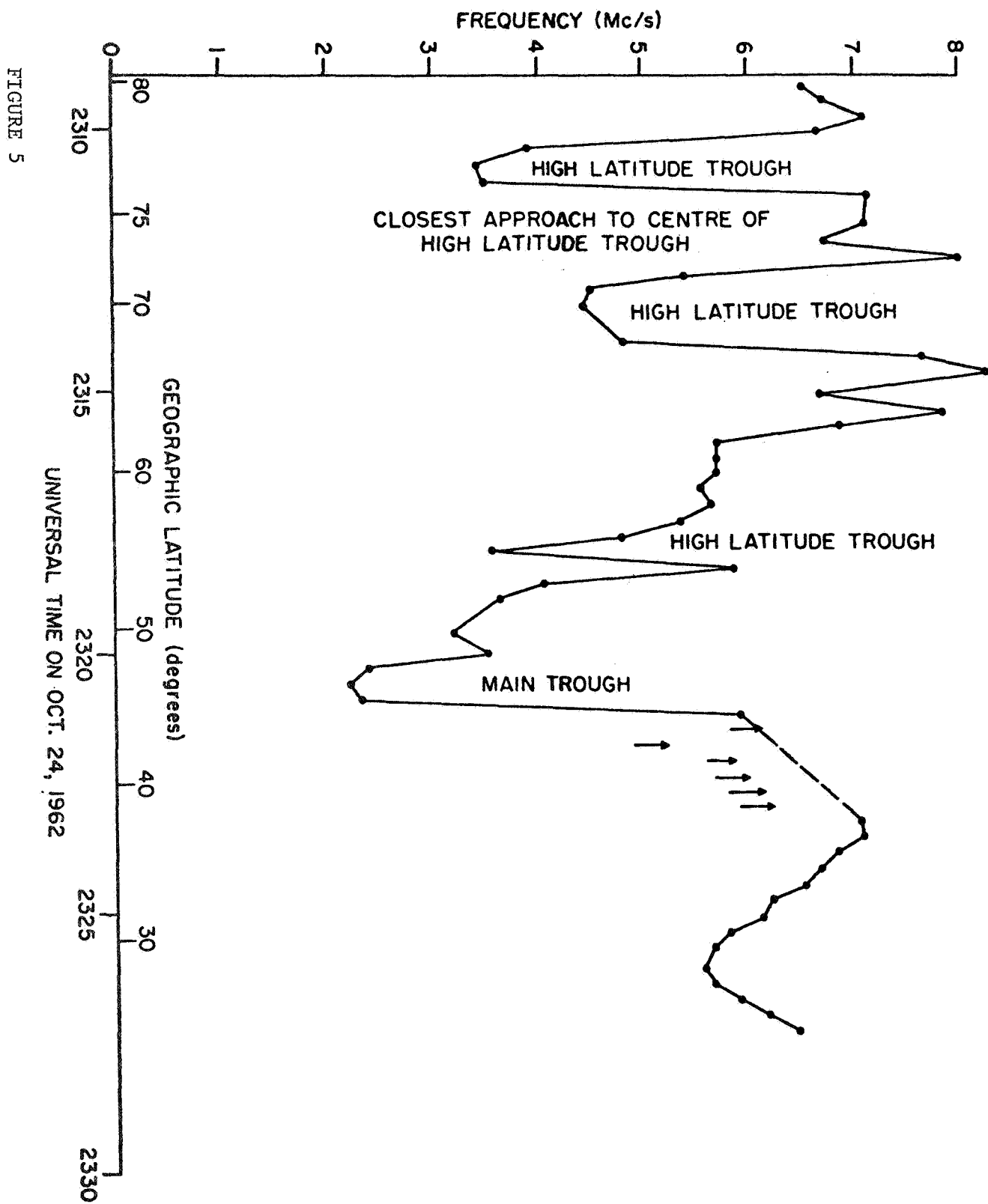


FIGURE 5

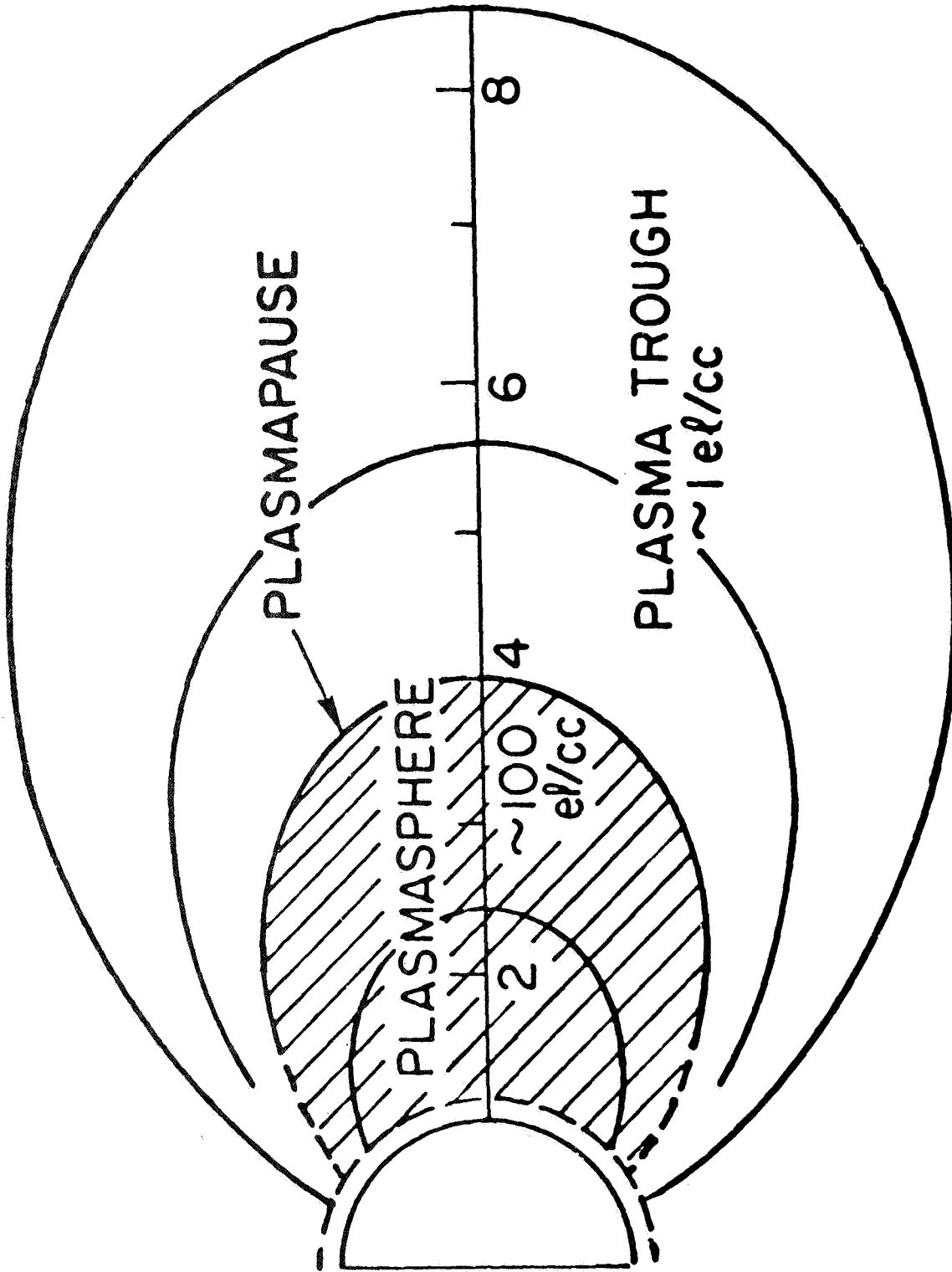


FIGURE 6

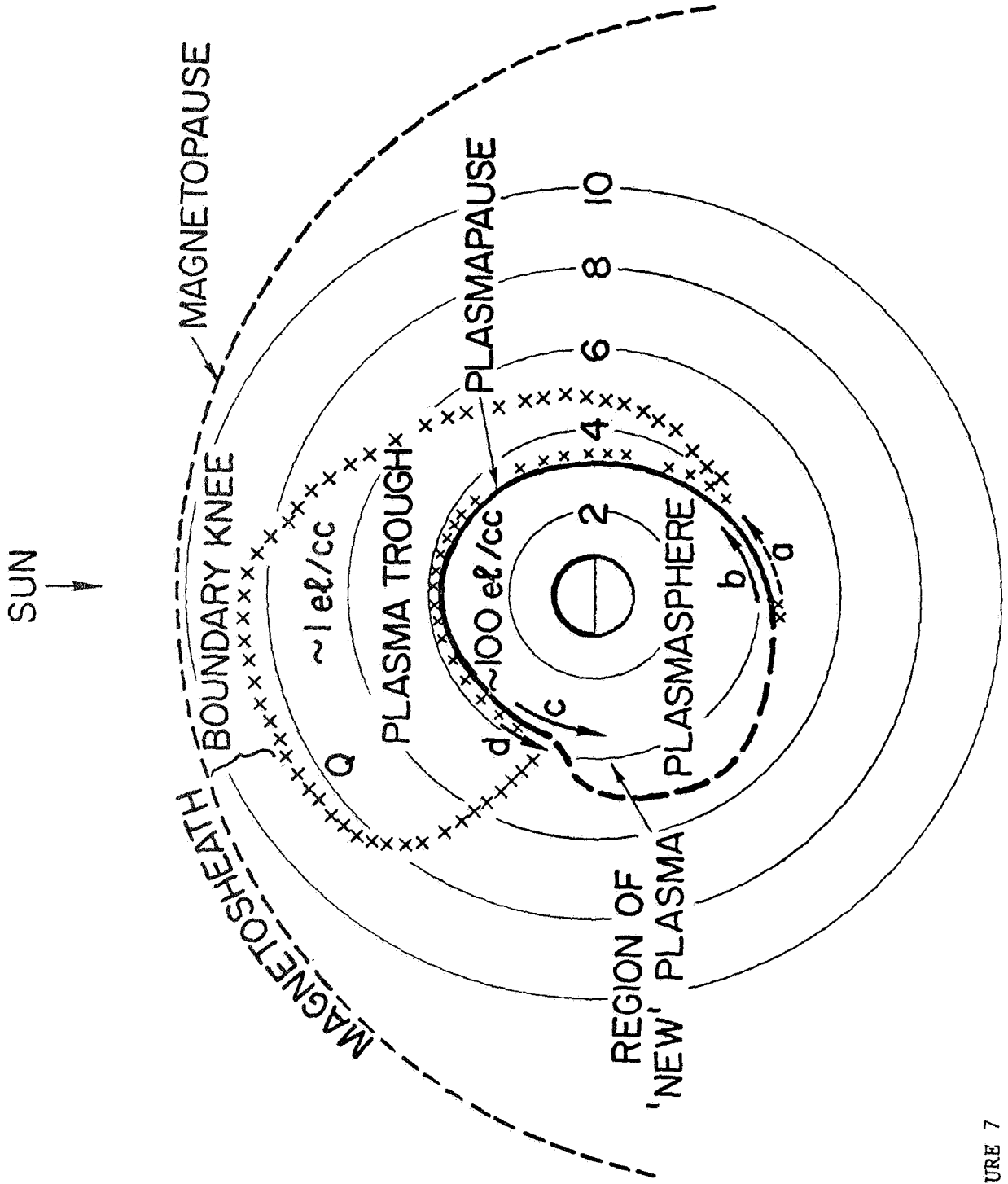


FIGURE 7

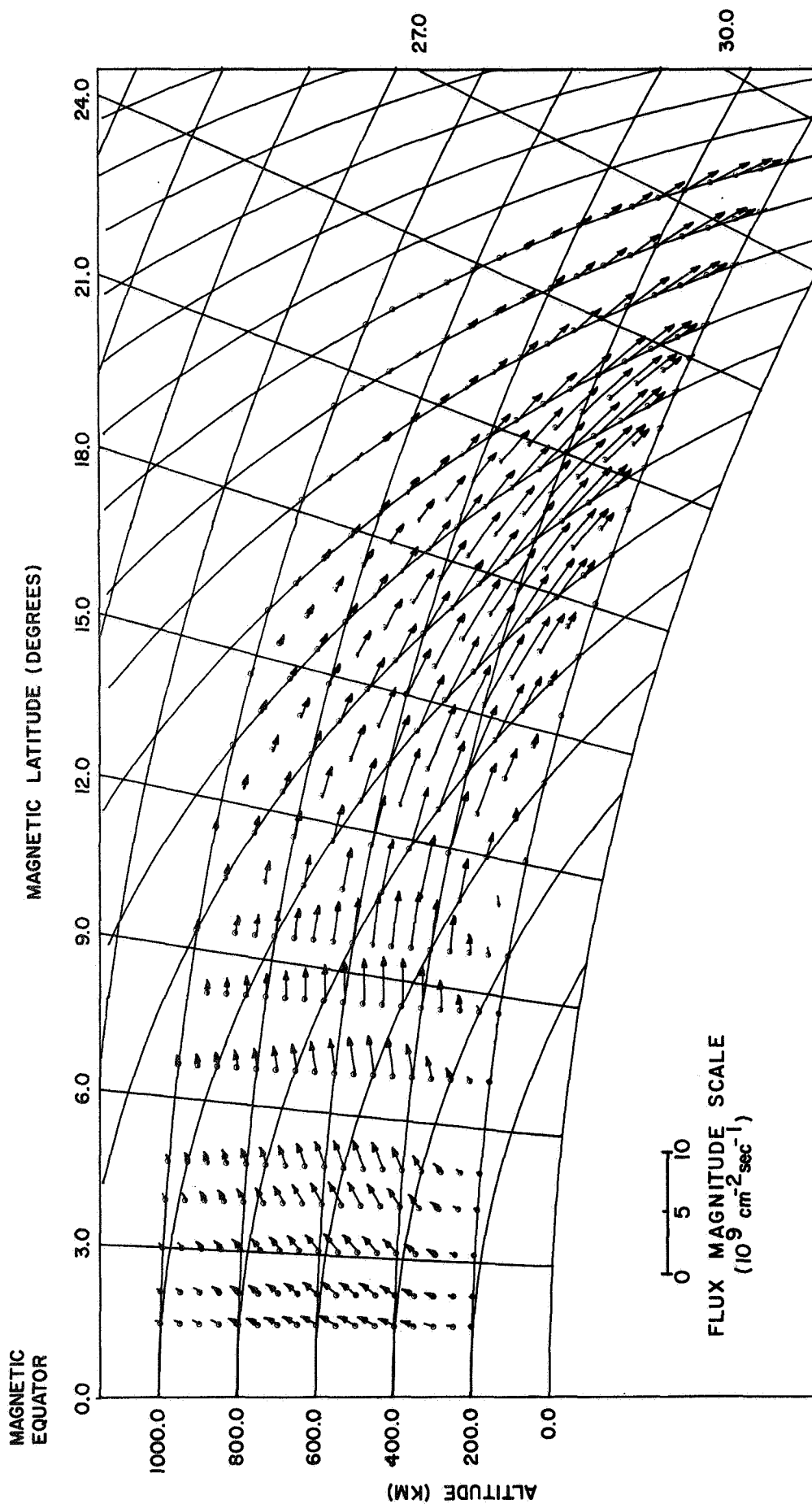


FIGURE 8

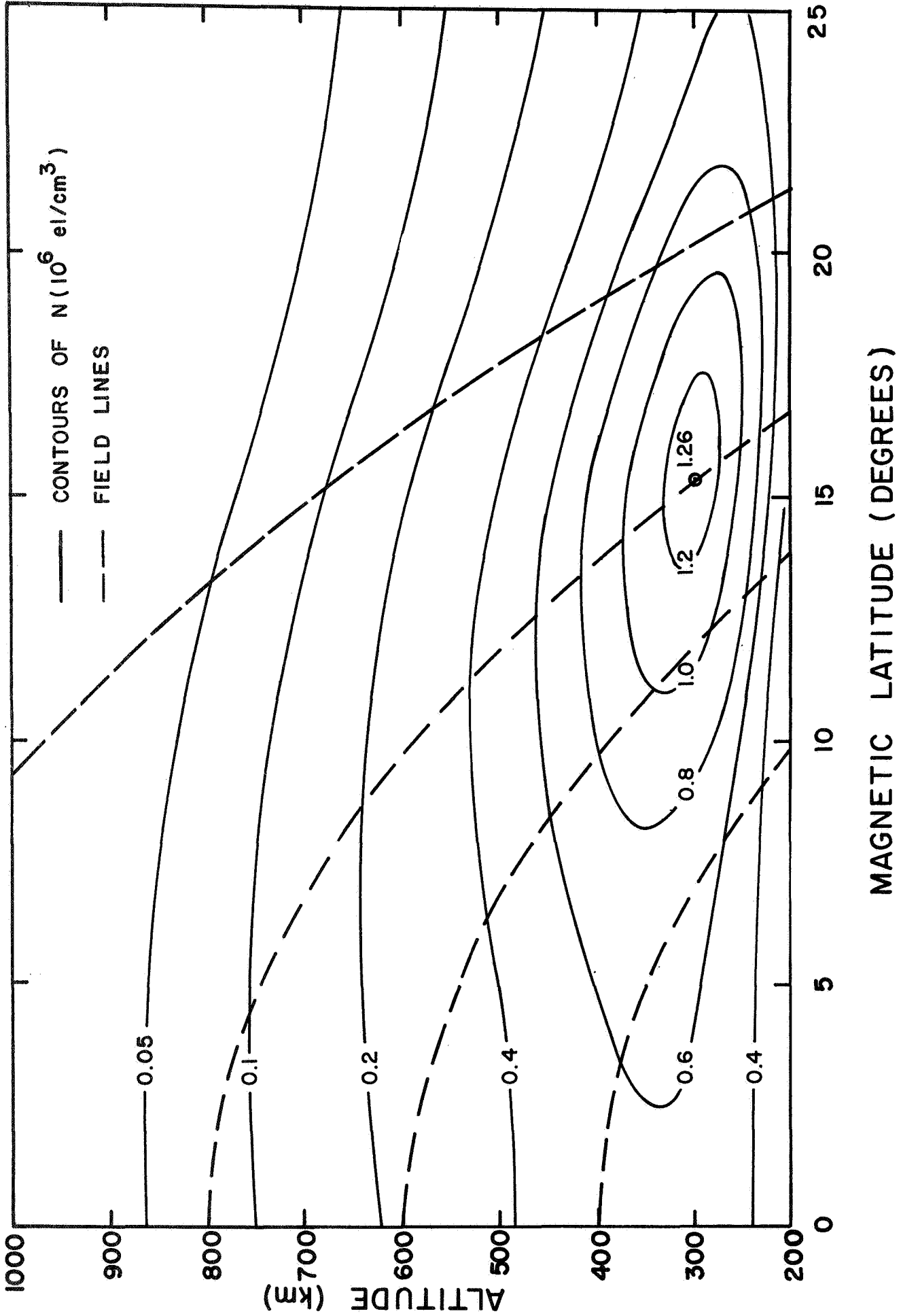


FIGURE 9

# Rocket Observations of Sporadic $E$ and Related Features

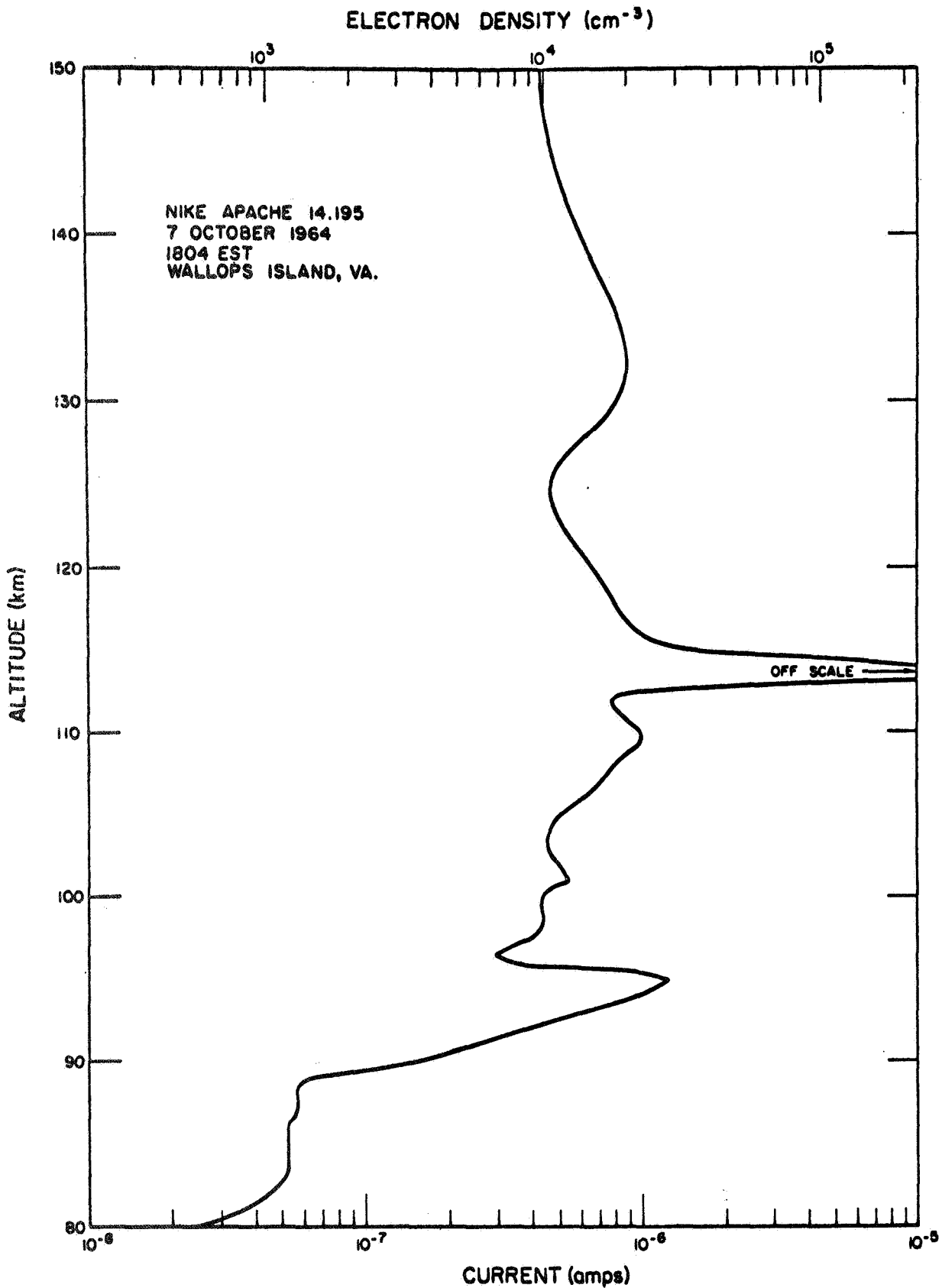


FIGURE 10

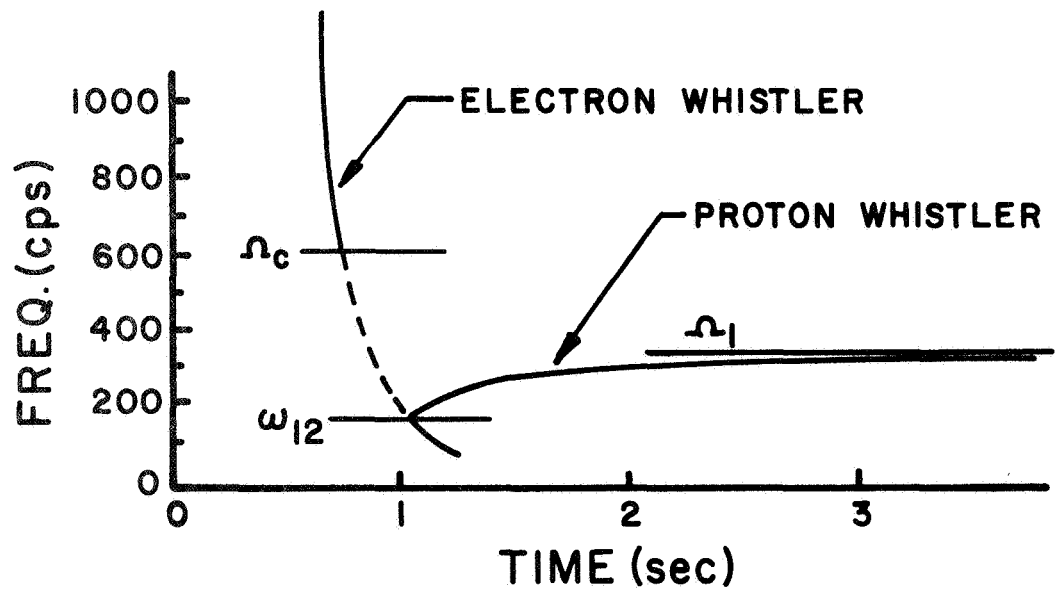


FIGURE 11



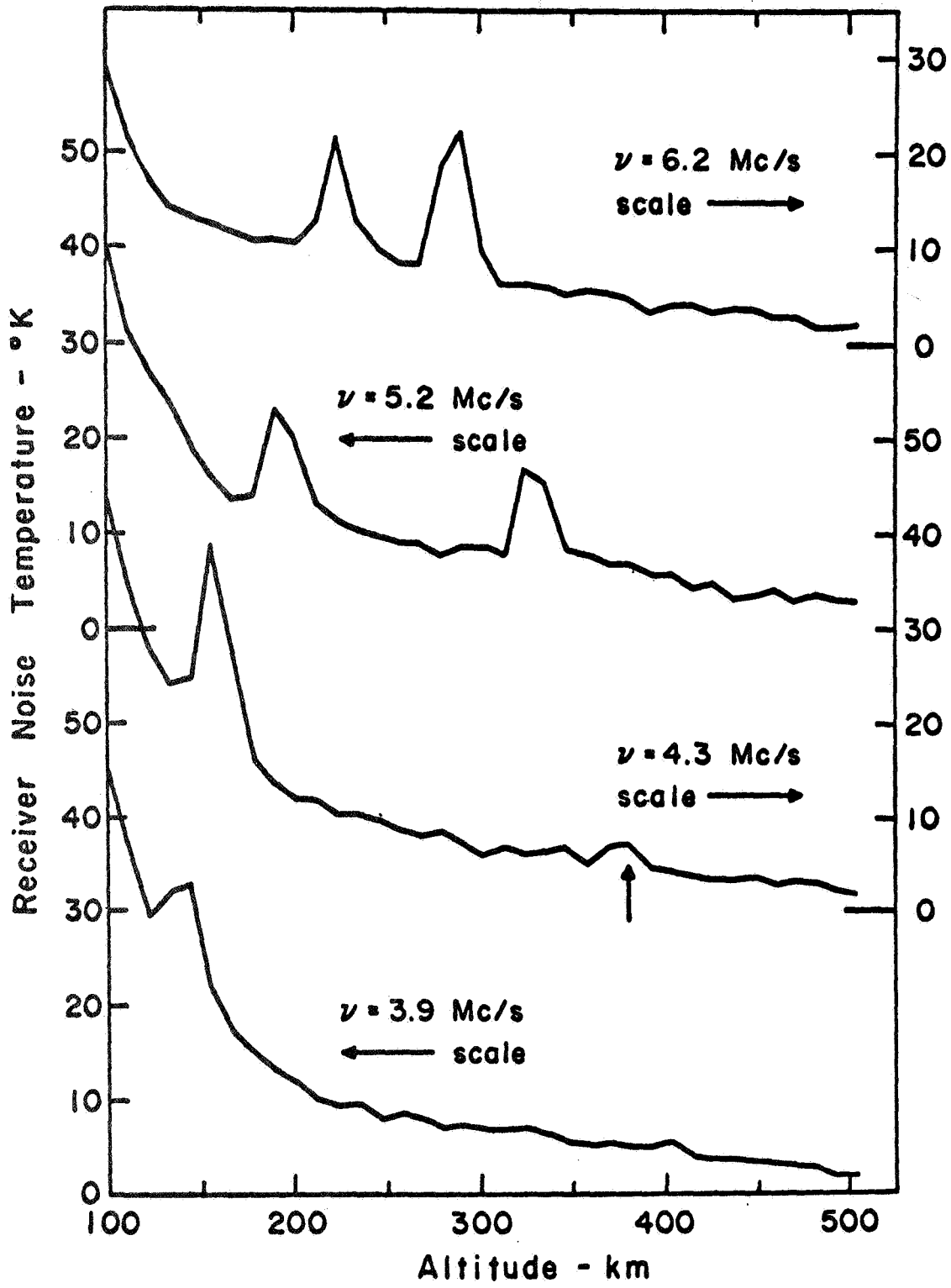


FIGURE 12